Journal of the European Ceramic Society **6** (1990) 243–251

Oxidation by CO–CO_2 of Dolomite–Carbon Refractories

X. Le Coq, F. Jeannot, B. Dupre, C. Gleitzer

Laboratoire de Chimie du Solide Minéral, Unité associée au CNRS n° 158,
Université de Nancy I, BP 239, 54506 Vandoeuvre-les-Nancy Cedex, France

F. Scheidt & P. Tassot

Institut de Recherche de la Sidérurgie, BP 320, 57214 Maizieres-les-Metz Cedex, France

(Received 19 February 1990; revised version received 11 April 1990; accepted 26 April 1990)

Abstract

Eight industrial samples, provided by three different suppliers, have been characterized for composition, phase analysis and texture. They differ by the binder nature (pitch or resin) and by the addition in some samples of 4–8% graphite.

The samples were oxidized (after pyrolysis) in CO–CO_2 mixtures at 1000–1400°C, and the reaction kinetics were recorded. Graphite-containing samples have a better resistance due to the lower reactivity of graphite compared to binder-carbon, as also shown by slow heating in CO_2. For a given supplier, resin-bonded samples are better than pitch-bonded.

The kinetics at 1200°C, with five different CO–CO_2 mixtures, were analysed with the two-dimensional (graphite) or three-dimensional (carbon) shrinking core model. This yields rate constants which obey the Langmuir–Hinshelwood pressure relation; accordingly there is no simple reaction order.

Acht kommerzielle Proben, die von drei verschiedenen Produzenten zur Verfügung gestellt wurden, wurden auf ihre Zusammensetzung, ihre kristallinen Phasen und Gefüge untersucht. Sie unterschieden sich durch die Art des Bindemittels (Pech oder Harz) und bei einigen Proben durch die Zugabe von 4–8% Graphit. Diese Proben wurden (nach einer Pyrolyse) in einer CO–CO_2 Atmosphäre bei 1000–1400°C oxidiert, wobei die Reaktionskinetik mitverfolgt wurde. Graphithaltige Proben zeigten, wie auch beim langsamen Aufheizen in CO_2, wegen der geringeren Reaktivität des Graphits gegenüber dem Kohlenstoff des Bindemittels eine höhere Oxidationsbeständigkeit. Bei gleichem Hersteller ergaben sich bei Harz gebundenen Proben bessere Werte als bei Pech gebundenen. Die Kinetik wurde bei 1200°C mit fünf verschiedenen CO–CO_2 Atmosphären nach dem Modell des abnehmenden Teilchendurchmessers (zweidimensional im Fall des Graphits oder dreidimensional im Fall des Kohlenstoffs) untersucht. Daraus resultierten Geschwindigkeitskonstanten, die der Langmuir–Hinshelwood–Druck–Gleichung folgen; dementsprechend liegt keine einfache Reaktionsordnung vor.

On a étudié la composition, les phases et la texture de huit échantillons industriels fournis par trois fournisseurs différents. Ils diffèrent par la nature du liant (poix ou résine) et par la teneur (de 4 à 8%) en graphite ajouté à certains échantillons. Après pyrolyse, on a mesuré la cinétique d'oxydation dans des mélanges CO–CO_2 à des températures variant entre 1000 et 1400°C. Les échantillons contenant du graphite présentent une meilleure résistance en raison de la réactivité du graphite qui est plus basse que celle du liant organique, ce qui est également montré lors d'un chauffage lent dans le CO_2. Pour un fournisseur donné, les échantillons contenant la résine sont meilleurs que ceux contenant la poix. La cinétique à 1200°C a été analysée pour cinq mélanges CO–CO_2 différents à l'aide du modèle du sphère contractante bi- (cas du graphite) ou tridimensionnel (cas du carbone). Les constantes de vitesse obtenues obéissent à la loi de Langmuir–Hinshelwood; il n'y a donc pas d'ordre de réaction simple.

Journal of the European Ceramic Society 0955-2219/90/$3.50

1 Introduction

The present trend towards high-purity steel necessitates complex treatments within ladles, the linings of which are subjected to intense corrosion by basic slags. Many European steelmakers have been led to the use of basic refractories of dolomitic type in secondary steelmaking and ladle refining processes.[1-3] Such dolomitic tempered refractories are mainly based on a sintered aggregate, actually composed of lime and magnesia, bound by a carbonaceous binder from pitch or resin.[4-6]

This classical material has been nearly the same for around ten years, as regards its application in ladles for steelmaking. But the recent addition of carbon to the magnesia refractories has led to the attempt of a similar step for dolomitic refractories. The potential interest of such a new material has been demonstrated in steel shops. However, the lack of knowledge of the corrosion mechanisms of the aggregate, and of the oxidation of the carbonaceous phase by gases and slags, limits the applications.

However, if the addition of carbon to doloma has several advantages, better resistance to thermal shock and to corrosion by slags, it has of course a drawback: its sensitivity to oxidation.

Few publications have been previously devoted to oxidation of carbon by CO_2 in these dolomite–graphite refractories. Palin and Richardson[7] have shown that in the oxidation of tar-bonded dolomite by oxygen at about 800°C, the CO_2 produced may react with lime. But this is a very limited aspect of the oxidation behaviour in these refractories. Therefore an investigation of the oxidation in CO–CO_2 mixtures has been undertaken, so approaching the conditions of the steelmaking plant, and several industrial samples have been compared, in order to see how differences in composition, porosity, texture, etc., may play a role in the resistance of these materials toward oxidizing atmospheres. The ultimate aim of this study is to understand the mechanism working in this solid–gas reaction, in other words how the driving force is shared between the chemical and diffusional steps, because this would indicate what kind of improvement is needed for a better resistance to oxidation.

Table 1. Chemical analysis (%) of the different doloma (on calcined materials). Data from the suppliers

Suppliers	*Samples*	*CaO*	*MgO*	*SiO_2*	*Fe_2O_3*	*Al_2O_3*
X	A, B	57–58	39–40	1·3	0·7	0·8
Y	C, D	58	39·5	1	0·7	0·8
Z	E, F	<61	>36	<1·5	<1	(+Mn_3O_4)
	G, H					<1

2 Materials

2.1 Composition

Eight samples, provided by three European suppliers, have been investigated. For each supplier there are several samples, depending on the binder nature (pitch or resin) and on the possible addition of graphite. The doloma composition, as given by the suppliers, is indicated in Table 1; obviously the three aggregates have comparable compositions and purities. The binder nature and graphite addition are given in Table 2; therefore there are two classes of refractories, with and without graphite, and the total carbon content, after pyrolysis of the binder (see Section 3.1), is either between 2·6 and 3·8% (samples A, E, F) or between 7·6 and 11·6% (B, C, D, G, H). The purity of the graphite addition has been tested by the electron microprobe and the scanning electron microscope techniques. As usual, the

Table 2. Main specifications of the samples

Suppliers	*Symbol*	*Binder nature*	*Addition of graphite?*	*Loss of weight during coking*[a]			*Residual carbon after coking*[a]		
				$\Delta m/m$ (%)	σ	n	(%)	σ	n
X	A	Resin	No	3·0	0·4	16	3·8	0·3	13
	B	Resin	Yes	2·8	0·4	17	11·6	0·7	11
Y	C	Pitch	Yes	2·6	0·2	29	9·5	0·3	16
	D	Resin	Yes	2·3	0·1	21	8·5	0·3	9
Z	E	Resin	No	2·0	0·1	15	3·2	0·2	17
	F	Pitch	No	2·6	0·1	13	2·6	0·1	12
	G	Resin	Yes	2·5	0·1	29	7·6	0·2	24
	H	Pitch	Yes	3·4	0·4	10	8·8	0·5	13

σ, Standard deviation, n, number of measurements.
[a] Measurements carried out in this laboratory.

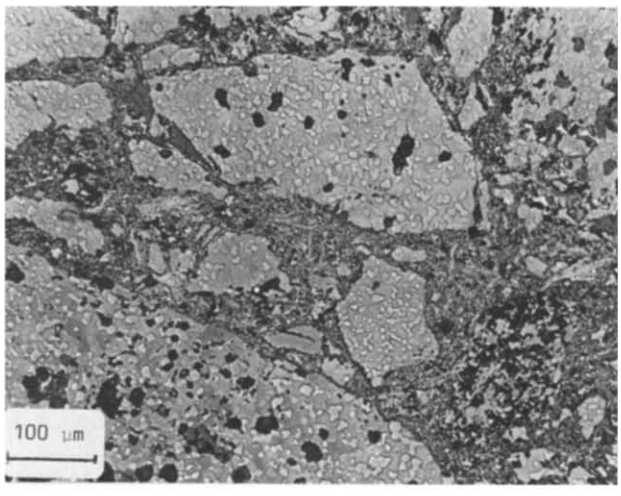

Fig. 1. Cross-section of sample E after coking.

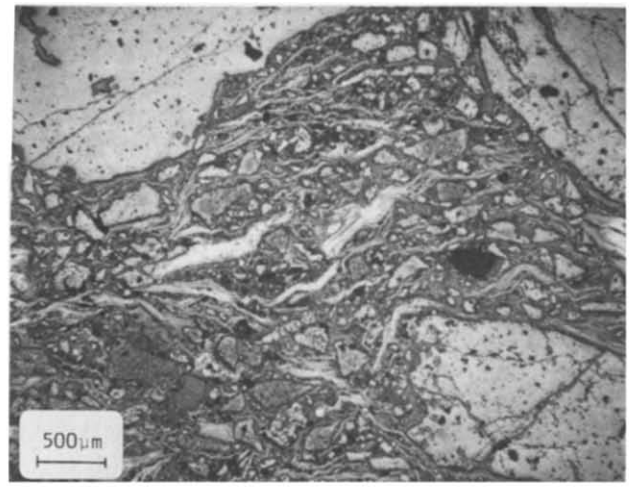

Fig. 2. Cross-section of sample B after coking.

natural graphites contain some impurities: mica, quartz, clays etc. However, a quantitative determination of these impurities is difficult: dissolution of dolomite in acids may also attack these phases at least partly.

2.2 Morphology

As seen from the optical microscope (Fig. 1) the samples show large doloma grains embedded in finer particles. When graphite has been added, it appears as lamellar flakes (Fig. 2) sometimes adapted to the aggregate thanks to their great deformation ability. Concerning the doloma grains, their diphasic character is clearly visible on Mg and Ca electron microprobe maps which moreover show that it is a calcium oxide matrix with MgO inclusions in the range 10–50 μm.

However, the size and geometry of these graphite flakes vary significantly from one sample to the other, with an average size of about 150 μm length and 20 μm width when seen in profile; therefore they are considered as disks with a radius $r_0 = 75\ \mu$m and a height of 20 μm.

2.3 Physical properties

The physical properties are gathered in Table 3, from which it appears that the cold crushing strength depends on the binder (it is better with resin than with pitch) and on the presence of graphite which, as expected, decreases the mechanical qualities. From room temperature up to 300°C the mechanical strength is higher for resin-bonded dolomite as for the standard pitch dolomite (due to the high volatile species ratio in the pitch, and also to the different structure of the carbon obtained from the two binders). Between 300 and 900°C, the mechanical properties of the pitch-bonded dolomite are worse than those of the resin-bonded dolomite due to the non-full polymerization of the carbon skeleton.

Table 3. Physical properties of the samples

Suppliers	*Samples*	*Apparent specific density* (g/cm^3)[a]	*Open porosity* (%)[a]	*Cold crushing strength* (N/mm^2)[a]	*Open porosity after coking 5 h, 1 000°C*
X	A	2·96	3–4	>55	14[b]
X	B	2·65	3–5	>25	21·6[c]
Y	C	2·82	4	22	16·9[c]
Y	D	—	—	—	14[a]
Z	E	2·90	5·3	100	11·3[b]
Z	F	2·95	3·7	50	11·3[b]
Z	G	2·70	10·0	60	14·5[b]
Z	H	2·85	5·5	27	12·4[b]

[a] Data from the suppliers.
[b] Measurements carried out at CRDM (Centre de Recherche de la Métallurgie, SOLLAC, Dunkerque).
[c] Measurements carried out at LRM (Laboratoire de Réfractaires et Minerais, Nancy).

3 Experimental

3.1 Pyrolysis

Before oxidation, it is necessary to eliminate the volatile species from pitch or resin. For this, the samples are heated up to 750°C (5 deg/min) and annealed at 750°C for 4 h, in a stream of 5% H_2/95% N_2 purified from oxygen traces by copper at 400°C, and from water vapour by P_4O_{10}.

The resulting weight losses are given in Table 2 and compared with the weight losses resulting from oxidation at high temperature. It has been checked that no additional weight loss is observed by pyrolysis at higher temperatures such as 900°C; this is in agreement with the TGA experiments of Lemon[8] on phenolic resins.

3.2 Oxidation

Samples cut as parallelepipeds of $1{\cdot}5 \times 1{\cdot}5 \times 3\,cm^3$ are put in an alumina crucible with many holes allowing a good flow of the gas, and heated in a thermal balance up to the desired temperature at 300 deg/h; this is done in a gas supposed to be inert towards the sample. However this condition is difficult to fulfil as

- —with N_2 or Ar, some oxidation takes place, even if these gases are passed over copper at 400°C resulting in an oxygen partial pressure of about 5×10^{-6} atm;
- —with 95% N_2/5% H_2 or 99% N_2/1% CO, there is some inner interaction, inside the sample, between MgO and carbon, yielding whiskers of MgO at its surface (MgO and C react to provide gaseous magnesium which is reoxidized by the traces of oxygen in the gas); moreover the platinum suspension is corroded, so that the first drawback (partial carbon oxidation during heating) being considered as less troublesome, the sample is heated in nitrogen, and consequently, if the origin of time is fixed to the moment when the CO–CO_2 mixture is admitted, the corresponding fractional conversion of the solid α is not zero, because, as mentioned above, the oxygen traces in nitrogen have already slightly oxidized the sample.

4 Oxidation of Graphite-free Samples

The kinetic results are exemplified by Fig. 3 for sample E at 1200°C, for several CO–CO_2 ratios (comparison between samples A, E and F gives E > F > A, from the best to the worst, in terms of their resistance to oxidation at 1000 and 1200°C in 50% CO–50% CO_2 mixtures). The small reacted fraction at $t = 0$, due to the oxidation during heating under 'neutral' atmosphere (as previously mentioned) has been corrected as follows: the overall curves α versus t have been fitted with polynomials, in such a way that the correlation coefficient is always better than 0·9998, and then extrapolated to $\alpha = 0$ yielding the network of curves of Fig. 3; it is claimed that this procedure is not only correct, but probably safer than the usual with a 'true' zero which always includes many errors.

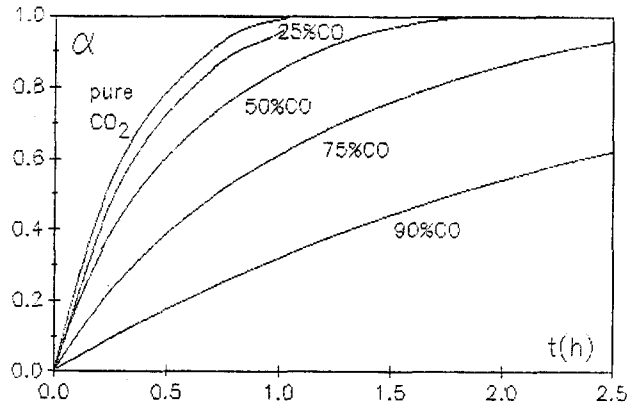

Fig. 3. Reacted fraction in the oxidation of sample E for $p_{CO_2} = 1$, 0·75, 0·5, 0·25 and 0·1 bar (total pressure 1 bar) at 1200°C.

Then, to analyse these curves, there are several treatments.

(1) The complete and rigorous treatment considers the porous solid and the time needed for the following three steps: the interfacial chemical reaction, the diffusion of reactants through the pores and through the boundary layer. Thus care has been taken to ensure that the gas supply was sufficient, through large variation of the gas flow, and also of the sample mass,[9] confirming that the boundary layer is not a barrier. As regards the pore-diffusion regime, it has been often observed in such cases;[10] however, it is stressed that most authors have dealt with oxygen, thus with faster reactions where the diffusional steps were more easily ruling the overall rate; analytical expressions have been given for a complete treatment for the case when the kinetics are first-order with respect to the reactant gas;[11] but it is known that this is not the general case in the oxidation of carbon, where most authors have found that the rate of gasification can be represented by an equation of Langmuir–Hinshelwood type:[12]

$$V = k_1 p_{CO_2} / (1 + k_2 p_{CO} + k_3 p_{CO_2})$$

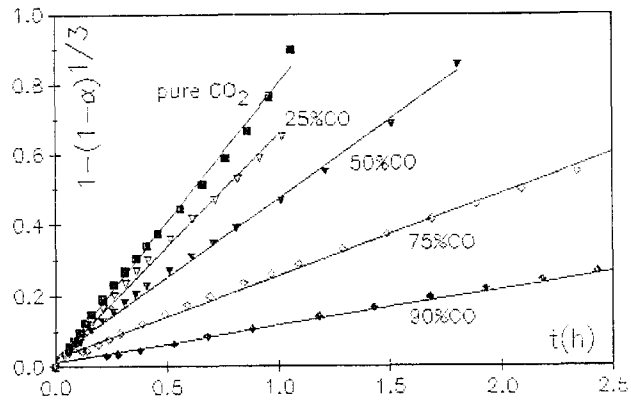

Fig. 4. $1-(1-\alpha)^{1/3}$ versus time, calculated from Fig. 3 data.

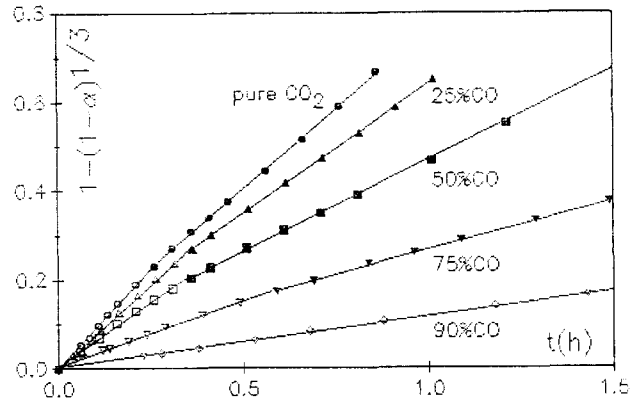

Fig. 5. As Fig. 4, but with division in 2 steps.

and in this case the generalized gas–solid rate equation, which takes into account the reaction and the various diffusions, is much more complicated, particularly here, with a solid which is a parallelepiped. Then, the only circumstance where this equation is simple, is the case when all diffusions are rapid enough, so that the chemical step is ruling the overall kinetics. Therefore the authors tried to apply the simplest chemical model, the so-called shrinking core model, which considers the carbon particles as quasi-spherical:

$$1-(1-\alpha)^{1/3} = kt/r_0 d$$

where α = reacted fraction; r_0 = initial radius of the particles; $d = 7{\cdot}9 \times 10^3$ mol C per m^3 (for a density $\sim 2{\cdot}95 \times 10^3$ kg/m^3); k = rate constant; depends on the gas composition.

As shown by Fig. 4 and Table 4, the fit of the experimental data is acceptable since the correlation coefficient CC is always better than 0·997; however it is also noted that a better fit is obtained if the α range is divided in two parts, as shown by Fig. 5 and Table 4, where the correlation coefficient is now near to or better than 0·999. (Nevertheless the significance of the second regime, at high α values, is not clear, because it is usually ascribed to a mixed regime of reaction and diffusion, but the linear character is connected to a sphere geometry.) The variation of the rate constant versus p_{CO_2} has been represented in Fig. 6, and fitted with a Langmuir–Hinshelwood equation, which yields:

$$\frac{k}{r_0} = \frac{2{\cdot}25\, p_{CO_2}}{1 + 0{\cdot}30\, p_{CO_2}} \quad (\text{C mol/m}^3\,\text{s})$$

The fact that $k_2 = 0$ in the Langmuir–Hinshelwood equation is consistent with the decrease of the reverse Boudouard reaction when temperature increases, and with the results from Ref. 13 for instance.

(2) Another, much simpler treatment can be applied following Turdogan and Vinters[14] who just consider the initial slope of α versus t, which is nothing else than $3k/r_0$ in the above treatment. Then these authors looked for a reaction rate order by plotting log ($d\alpha$/dt) versus log p_{CO_2} and found that while at $p_{CO} = 0$ the rate is proportional to $p_{CO_2}^{1/2}$, in the presence of CO, at a fixed value of p_{CO}, the rate is proportional to p_{CO_2}.

If log (k/r_0) versus log p_{CO_2} (Fig. 7) is drawn, it is found that the data are fairly well aligned

Table 4

P_{CO_2}	k/r_0	CC	k'/r_0	CC	k''/r_0	CC	α_t
1·00	1·73	0·997 8	2·00	0·999 2	1·58	0·999 8	0·50
0·75	1·40	0·997 7	1·67	0·999 1	1·25	0·999 8	0·65
0·5	0·99	0·998 0	1·25	0·888 2	0·90	0·999 7	0·50
0·25	0·50	0·998 4	0·65	0·998 5	0·48	0·999 6	0·45
0·1	0·22	0·998 4	0·24	0·999 4	0·20	0·999 9	0·00

P_{CO_2} in bar.
k/r_0 in C mol/m^3 s.

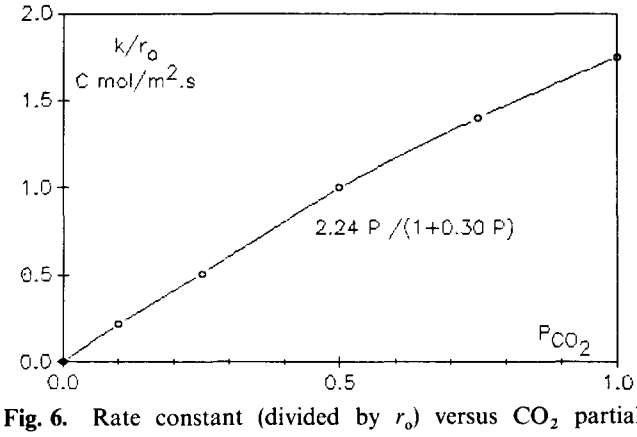

Fig. 6. Rate constant (divided by r_0) versus CO_2 partial pressure.

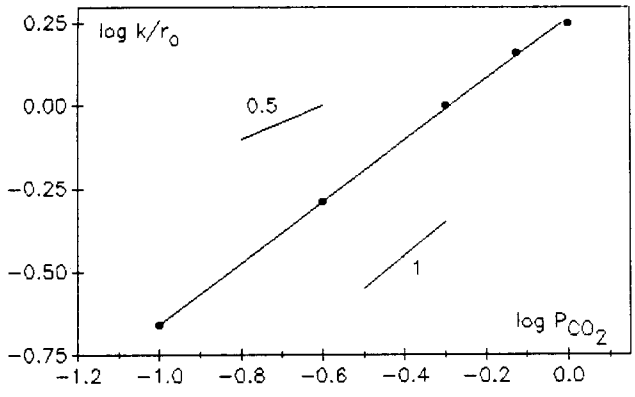

Fig. 7. As Fig. 6 but with logarithms.

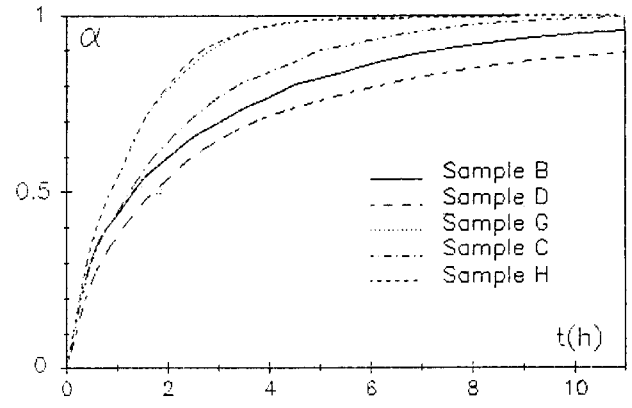

Fig. 8. Comparison of the five graphite-containing oxidized samples at 1200°C with $p_{CO} = p_{CO_2} = 0{\cdot}5$ bar.

(correlation coefficient 0·9997) with a slope slightly less than one (0·91). However the authors wish to stress that, if the Langmuir–Hinshelwood equation applies, no simple order of reaction can exist.

5 Oxidation of Graphite-containing Samples

5.1 Comparison of the different samples in isothermal oxidation

The samples were oxidized under standard conditions ($CO/CO_2 = 50/50$, total pressure 1 bar, $T =$ 1100, 1200 and 1400°C). The results at 1200°C for instance are shown in Fig. 8; clearly the samples G and H are more readily oxidized, even if the differences tend to vanish at higher temperature. The rankings are D > B > C > G > H and Y > X > Z.

It is worth stressing that no correlation appears with the porosity after coking, but, for a given supplier, resin-bonded samples are better than pitch-bonded. Actually it must be recalled that no detailed information is available on the graphite purity, which may play a role in this ranking.

5.2 Carbon reactivity

Such a test is obtained by recording the weight loss in the oxidation by O_2 or CO_2 with a heating rate of 50 deg/h. The results obtained with CO_2 are given in Fig. 9.

Samples B and D, which are the best according to Fig. 8, are more easily oxidized at low temperature, especially sample B. This means that the carbon from the binder is more reactive in these samples, as it burns first, and the graphite afterwards, even if these two steps have some overlapping. However it is clear that in the second step, roughly corresponding to the range 0·4–1·0, the average slope of the B curve is smaller than for other samples, and the same is true, to a lower extent, for sample D; this means that the graphite of sample B is significantly less reactive than the others; it may even be stated that, if sample B has a better binder (providing a carbon of reactivity comparable to the other samples) it would resist oxidation much better.

On the other hand, it seems difficult to account for the poor behaviour of samples G and H. They clearly profit by good binders, especially sample H. Then, in order to clarify this point, cross-sections of samples B, C and G are shown; it appears (Fig. 10) that the graphite flakes are less lamellar in sample G; this may explain its higher reactivity, as it is well known that the reaction proceeds mainly from the sheets' lateral surfaces,[12] as illustrated by Fig. 11. However it must be again recalled that graphite purity is unknown and might also play a role.

5.3 Kinetics

This has been investigated on sample G, the oxidation of which is represented by Fig. 12 for $T =$ 1200°C; these curves have been corrected, for the preliminary oxidation, as before (Section 4), with correlation coefficients better than 0·999.

Obviously the carbon coming from the resin burns more rapidly than the graphite. Thus from the

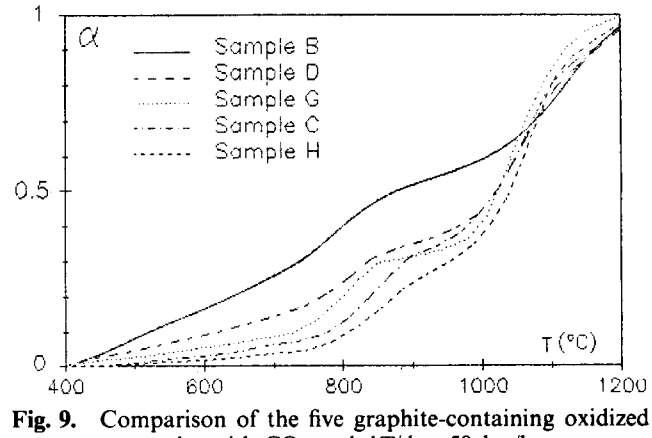

Fig. 9. Comparison of the five graphite-containing oxidized samples with CO_2 and $dT/dt = 50$ deg/h.

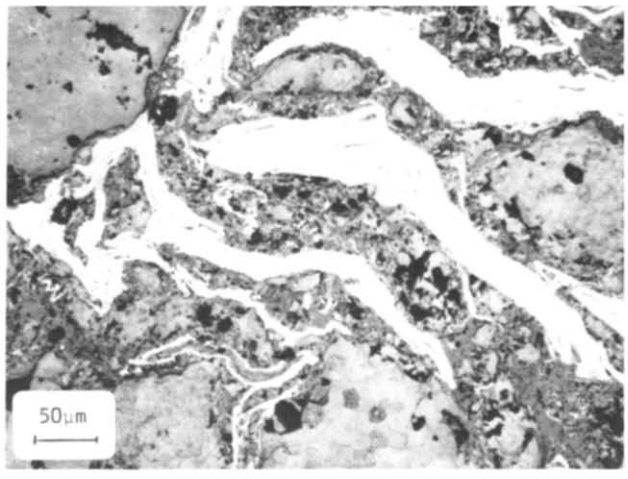

(a)

(b)

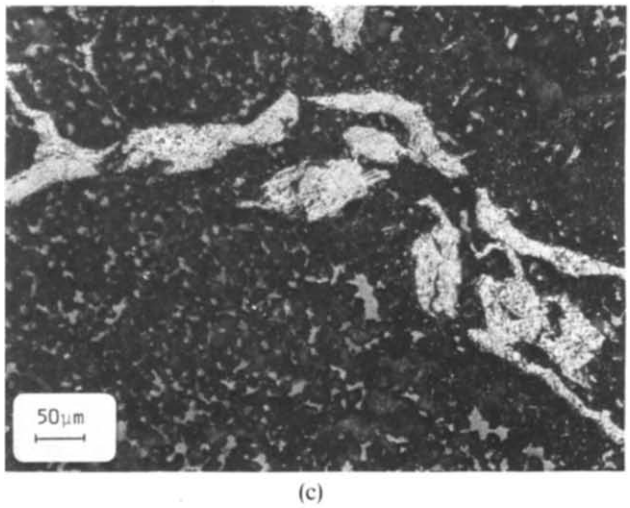

(c)

Fig. 10. Cross-sections of samples B (a), C (b) and G (c).

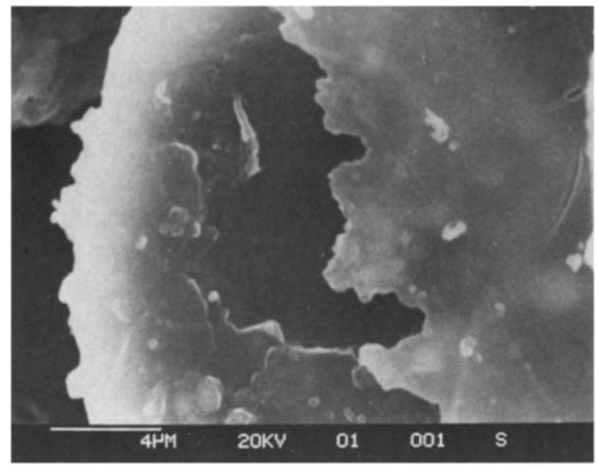

Fig. 11. Scanning electron microscope view of partially oxidized flakes of pyrolysed sample G.

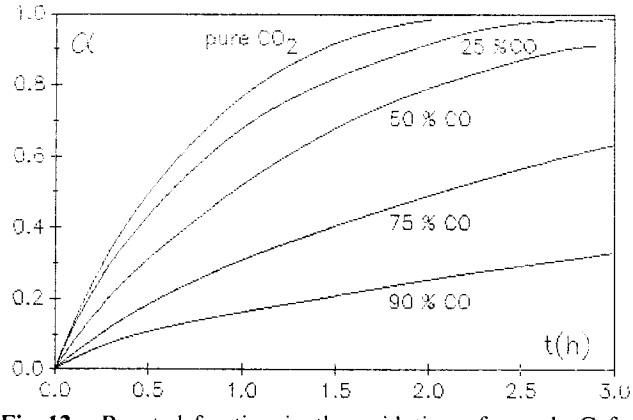

Fig. 12. Reacted fraction in the oxidation of sample G for $p_{CO_2} = 1$, 0·75, 0·5, 0·25 and 0·1 bar (total pressure 1 bar) at 1200°C.

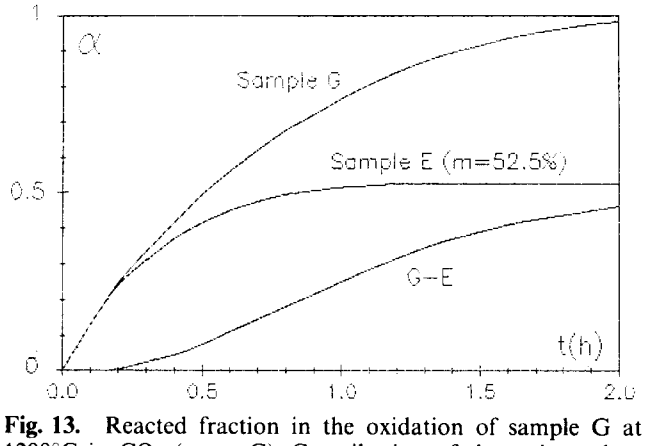

Fig. 13. Reacted fraction in the oxidation of sample G at 1200°C in CO_2 (curve G). Contribution of the resin–carbon calculated from sample E (curve E). Difference curve (G–E).

curve of sample G, the fraction corresponding to the oxidation of the resin carbon calculated from sample E (which is from the same supplier) can be deduced. As seen in Fig. 13, the resulting curve for graphite implies that its reaction is completely inhibited for about 10 min; conversely, the resin carbon has completely burnt in 1 h and the second hour corresponds to the oxidation of graphite only. However, it must be stressed that the above procedure is somewhat arbitrary as, in spite of the fact that the initial slope exactly corresponds to that of sample E, this might be fortuitous, and the case of mutual inhibition of the two oxidations cannot be disregarded; this is illustrated by Fig. 14 where the

time needed for the burn off of the resin carbon has been arbitrarily increased by 30%.

In order to find the graphite oxidation rate constant, the transformed curves $1-(1-\alpha)^{1/2} = kt/r_0 d$ have been calculated, because the graphite is considered as cylindrical flakes reacting along the lateral surface and this yields the 1/2 exponent.[5] Acceptable straight lines are thus obtained for the end of the reaction when the binder-carbon has burned off (Fig. 15), from which the rate constant can be calculated, as it is known here that $r_0 \sim 75\ \mu m$ (Table 5); however it must be noted that a fit with the

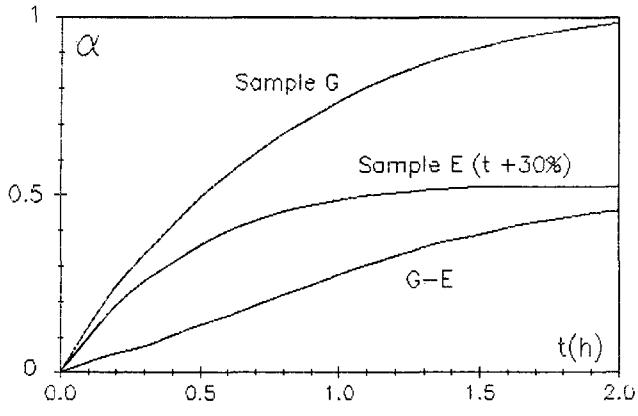

Fig. 14. As for Fig. 13 but the total reaction time for the resin carbon contribution has been increased by 30%.

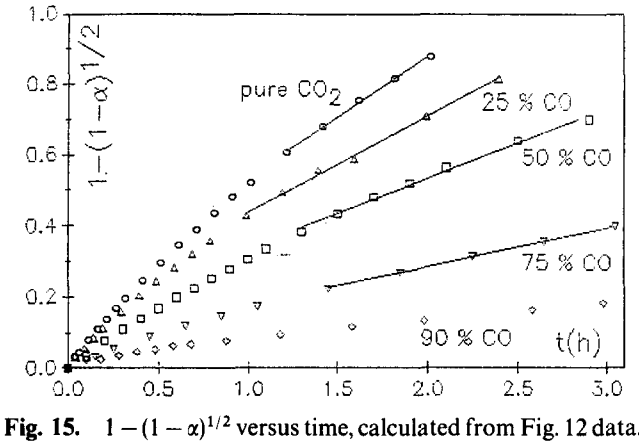

Fig. 15. $1-(1-\alpha)^{1/2}$ versus time, calculated from Fig. 12 data.

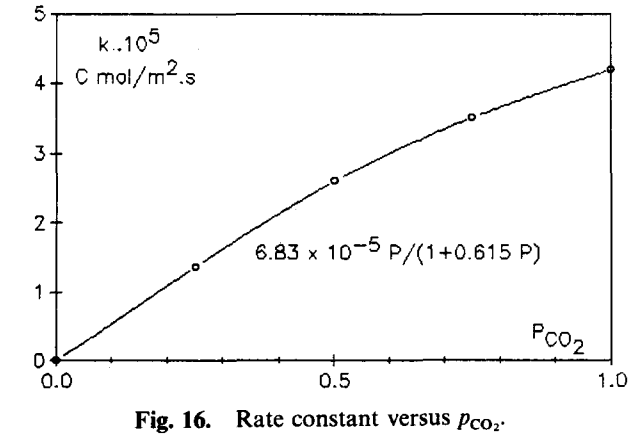

Fig. 16. Rate constant versus p_{CO_2}.

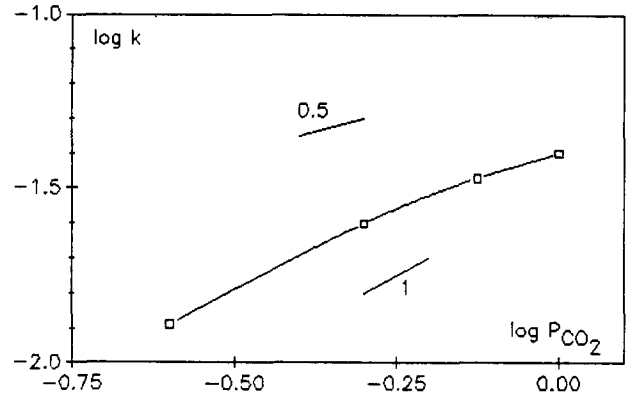

Fig. 17. As for Fig. 16 but with logarithms.

$1-(1-\alpha)^{1/3}$ equation would suit as well, but the first one is taken for physical reasons. As for sample E, it is found that the results may be represented by a Langmuir–Hinshelwood equation (Fig. 16):

$$k = \frac{6{\cdot}85 \times 10^{-5} p_{CO_2}}{1 + 0{\cdot}615 p_{CO_2}} \quad (\text{C mol/m}^2\,\text{s})$$

whereas the $\log k$ versus $\log p$ curve (Fig. 17) yields an apparent order in between 1 and 0·5.

6 Conclusions

Graphite is obviously a favourable additive in order to confer to pitch- or resin-bonded doloma a better resistance to oxidation by CO–CO_2. This is shown well by oxidation with a slow heating rate (50 deg/h) where two successive steps (with some overlap) are recorded at around 800 and 1100°C for oxidation of binder-carbon and of graphite respectively, in pure CO_2.

Second-order differences are noted among the two sets of samples (with or without graphite). Within a given set, and a given supplier, resin-bonded samples resist oxidation by 50% CO–50% CO_2 at 1200°C better than the pitch-bonded, in the order E > F, D > C, G > H, in spite of the fact that, in slow heating, the resin-carbon burns somewhat earlier than the pitch-carbon.

The kinetics of resin-carbon oxidation, at 1200°C

Table 5

P_{CO_2}	k	CC	$\alpha >$
1	$4{\cdot}15 \times 10^{-5}$	0·998 7	0·75
0·75	$3{\cdot}5 \times 10^{-5}$	0·998 3	0·65
0·5	$2{\cdot}6 \times 10^{-5}$	0·996 6	0·60
0·25	$1{\cdot}35 \times 10^{-5}$	0·999 6	0·40

P_{CO_2} in bar.
k in C mol/m² s (for $r_0 \sim 75\ \mu m$).

with five different CO–CO_2 mixtures, has been analysed with the shrinking core model; this yields a rate constant compatible with a Langmuir–Hinshelwood pressure dependence; accordingly there is no definite reaction order.

The kinetics of graphite-containing samples is much more complicated. After removal of the binder-carbon contribution, the two-dimensional shrinking core model has been applied, yielding again a rate constant obeying the Langmuir–Hinshelwood equation, with no simple reaction order.

Finally, in spite of the low differences noted among the different samples, a few recommendations are possible:

(1) Graphite addition is desirable, but with a reactivity as low as possible: extended lamellar flakes, and low iron content (it will be shown in a subsequent publication that iron catalyses the oxidation by CO–CO_2 even at 1200°C) are also desirable.

(2) Resin gives better results than pitch in spite of its early oxidation which suggests that fine carbon particles do not improve the high-temperature cohesion and rather may locally react with MgO.

Acknowledgement

This work has been supported by the Centre National de la Recherche Scientifique through a grant to X.L.C.

References

1. Stradtmann, J., Mlaker, G. & Thomas, R. C., Dolomitic refractories in secondary steelmaking and ladle refining processes. In *First Int. Conf. Refractories*, Tokyo, Japan, 15–18 November 1983.
2. Klages, G., Klein, A., Rubens, W. & Sperl, H., Bedeutung des heimischen Rohstoffs Dolomit für die Stahlerzeugung in der Bundesrepublik Deutschland. *Stahl u. Eisen*, **106** (1986) 1066.
3. Panek, Z., Danek, V. & Kley, G., Korrosion geschmolzener Feuerfestmaterialen des Systems MgO–CaO durch Konverterschlaken. *Silikattechnik*, **38** (1987) 56.
4. Stradtmann, J., Dolomite in modern metallurgy. *Metallurgical Plant and Technology*, **3** (1978) 42.
5. Baum, R. & Zörcher, H., Dolomite bricks in steel-works ladles, *Metallurgical Plant and Technology*, **4** (1978) 38.
6. Savchenko, Y., Kukuruzov, A., Perepelitsyn, V., Novoselova, L. & Shubin, V., Dolomite tar-impregnated refractories with a ceramic bond. *Ogneupory*, **26** (1985) 38.
7. Palin, F. & Richardson, H., A study of the oxidation temperature and amount of residual carbon in coked tarred magnesite and dolomite. *Trans. J. Brit. Ceram. Soc.*, **71** (1972) 37.
8. Lemon, P., Phenol formaldehyde polymers for the bonding of refractories. *Brit. Ceram. Trans. J.*, **84** (1985) 53.
9. Le Coq, X., Etude physico-chimique de matériaux réfractaires de type dolomite-carbone leur oxydation par les gaz et leur corrosion par un latier désulfuration. PhD thesis Nancy University, 1989.
10. Ozgen, O. S. & Rand, B., *Brit. Ceram. Trans. J.*, **84** (1985) 70, 213.
11. Szekely, J., Evans, J. W. & Sohn, H. Y. (eds) *Gas–Solid Reactions*, Academic Press, New York, 1976.
12. Lewis, J. B., Thermal gas reactions of graphite. In *Modern Aspects of Graphite Technology*, ed. L. Blackman. Academic Press, London, 1970, p. 129.
13. Strange, J. & Walker, P., Carbon–carbon dioxide reaction: Langmuir–Hinshelwood kinetics at intermediate pressures. *Carbon*, **14** (1976) 345.
14. Turkdogan, E. T. & Vinters, J. V., Effect of carbon monoxide on the rate of oxidation of charcoal, graphite and coke in carbon dioxide. *Carbon*, **8** (1970) 39.